

The British University in Egypt

BUE Scholar

Pharmacy

Health Sciences

2021

Targeting ROS-Dependent AKT/GSK-3 β /NF- κ B and DJ-1/Nrf2 Pathways by Dapagliflozin Attenuates Neuronal Injury and Motor Dysfunction in Rotenone-Induced Parkinson's Disease Rat Model

Marwa Safar
marwa.safar@bue.edu.eg

Follow this and additional works at: <https://buescholar.bue.edu.eg/pharmacy>

Recommended Citation

Safar, Marwa, "Targeting ROS-Dependent AKT/GSK-3 β /NF- κ B and DJ-1/Nrf2 Pathways by Dapagliflozin Attenuates Neuronal Injury and Motor Dysfunction in Rotenone-Induced Parkinson's Disease Rat Model" (2021). *Pharmacy*. 588.

<https://buescholar.bue.edu.eg/pharmacy/588>

This Article is brought to you for free and open access by the Health Sciences at BUE Scholar. It has been accepted for inclusion in Pharmacy by an authorized administrator of BUE Scholar. For more information, please contact bue.scholar@gmail.com.

Targeting ROS-Dependent AKT/GSK-3 β /NF- κ B and DJ-1/Nrf2 Pathways by Dapagliflozin Attenuates Neuronal Injury and Motor Dysfunction in Rotenone-Induced Parkinson's Disease Rat Model

Hany H. Arab, Marwa M. Safar, and Nancy N. Shahin*

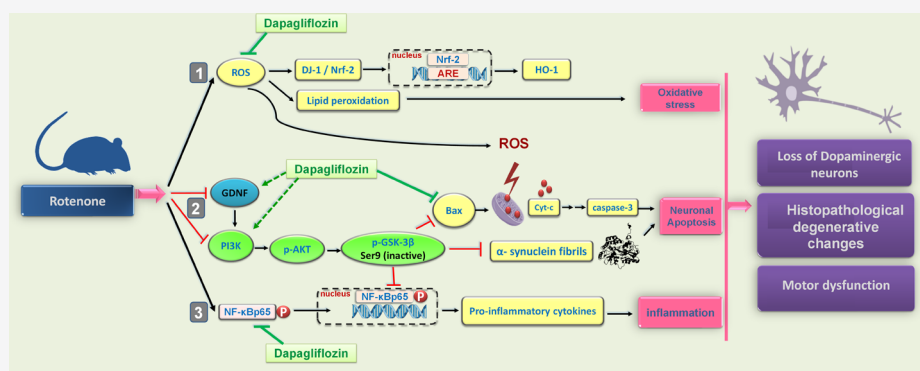
Cite This: <https://dx.doi.org/10.1021/acchemneuro.0c00722>

Read Online

ACCESS |

Metrics & More

Article Recommendations



ABSTRACT: Dapagliflozin, a selective sodium-glucose co-transporter 2 (SGLT2) inhibitor, has emerged as a promising neuroprotective agent in murine models of epilepsy and obesity-induced cognitive impairment through its marked antioxidant/antiapoptotic features. However, the impact of dapagliflozin on the pathogenesis of Parkinson's disease (PD) is lacking. Hence, the present study aimed at exploring the potential neuroprotective effects of dapagliflozin against PD-associated neurodegenerative aberrations/motor dysfunction in rotenone-induced PD rat model. Rotenone (1.5 mg/kg) was subcutaneously administered every other day for 3 weeks. The expression of target signals was investigated using qPCR, Western blotting, ELISA, and immunohistochemistry. Dapagliflozin (1 mg/kg)/day, by gavage for 3 weeks) attenuated PD motor dysfunction and improved motor coordination in the open-field and rotarod tests without triggering hypoglycemia. It also diminished the histopathologic alterations and α -synuclein expression and augmented tyrosine hydroxylase and dopamine levels. Dapagliflozin markedly alleviated neuronal oxidative stress via lowering lipid peroxides with consequent restoration of the disturbed DJ-1/Nrf2 pathway. Moreover, dapagliflozin counteracted ROS-dependent neuronal apoptosis and upregulated GDNF and its downstream PI3K/AKT/GSK-3 β (Ser9) pathway. Meanwhile, it suppressed neuroinflammation via curbing the activation of NF- κ B pathway and TNF- α levels. Together, these pleiotropic neuroprotective effects highlight the promising role of dapagliflozin in the management of PD.

KEYWORDS: Dapagliflozin, rotenone, neuroinflammation, AKT, GSK-3 β , Nrf2

INTRODUCTION

Parkinson's disease (PD) is the most common neurodegenerative movement disorder that affects the elderly.¹ The primary pathological hallmark of PD involves progressive and selective loss of dopaminergic (DA) neurons and accumulation of cytoplasmic protein aggregates known as Lewy bodies (LB) which comprise α -synuclein protein fibrils in several brain regions of PD patients.² When the number of DA neurons falls below 20–40%, the classical motor and behavioral disturbances of PD are manifested, e.g., bradykinesia, rigidity, resting tremors, and postural instability. Several genetic and environmental factors including the exposure to pesticides are involved in the pathogenesis of PD.³

The exact molecular mechanisms for PD pathogenesis are not well-defined. However, reactive oxygen species (ROS)-associated mitochondrial dysfunction/ATP depletion is a chief hallmark that mediates the selective loss of dopaminergic neurons in PD.³ Meanwhile, ROS-dependent apoptosis and neuronal inflammation have been reported to play crucial roles

Received: November 10, 2020

Accepted: January 29, 2021

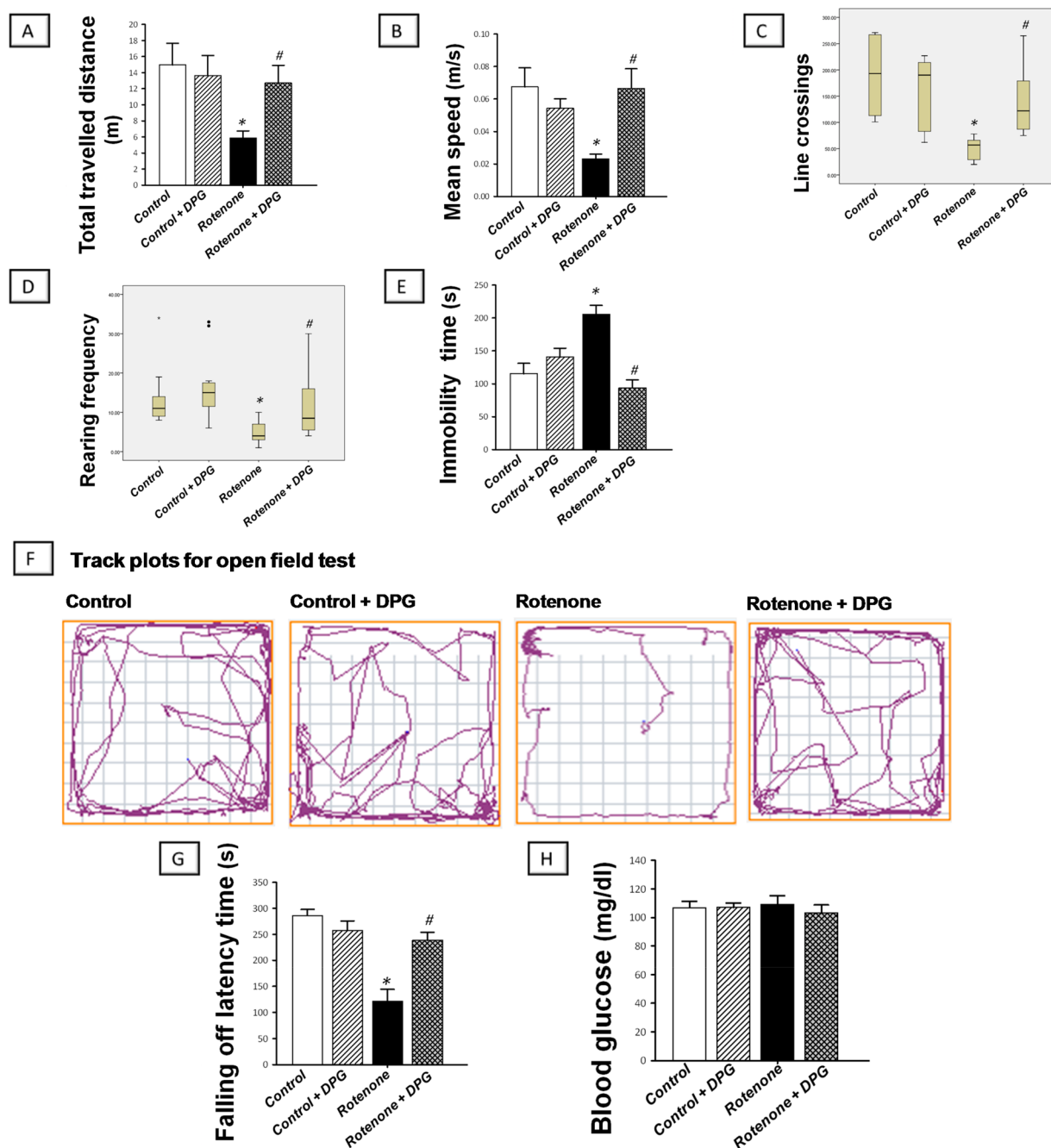


Figure 1. Dapagliflozin attenuates the motor dysfunction in rats with rotenone-induced PD. The motor performance was assessed by the open-field test, while the motor coordination was examined using the rotarod test. Rotenone was subcutaneously injected as 11 subcutaneous injections (1.5 mg/kg) every other day over 3 weeks span, while dapagliflozin (1 (mg/kg)/day) was given by the oral gavage daily over the same period. Open-field test: (A) total traveled distance; (B) mean speed; (C) line crossings; (D) rearing frequency; (E) immobility time; (F) representative track plots of rats during the open-field test. Rotarod test: (G) fall-off latency. (H) blood glucose levels. The parametric data (total traveled distance, mean speed, immobility time, fall-off latency, and blood glucose levels) are presented as the mean \pm SEM, while the nonparametric data (line crossings and rearing frequency) are presented as the median with interquartile range; $n = 6-10$; * $P < 0.05$, statistical significance against the control group; # $P < 0.05$, statistical significance against the rotenone group; DPG, dapagliflozin.

in the progression of PD.³⁻⁵ The phosphoinositide 3-kinase (PI3K)/protein kinase B (AKT) pathway has been characterized to play a pivotal role in regulating cell proliferation and survival. It has been established that the dysregulation of PI3K/AKT signaling is implicated in PD pathogenesis where low p-AKT levels have been described in the DA neurons of post-mortem PD patients.⁶ The glycogen synthase kinase-3 β (GSK-3 β) is a multifunctional kinase essential for various

cellular functions, such as cell proliferation, differentiation, and apoptosis. It plays a crucial role in PD pathogenesis where it serves as a proinflammatory/proapoptotic kinase downstream of the PI3K/AKT pathway. Of note, phosphorylation of GSK-3 β at Tyr216 has been reported to activate its proinflammatory/proapoptotic actions, whereas its phosphorylation at Ser9 has been reported to block these deleterious effects.³ In the context of neuroinflammation, GSK-3 β activates several

transcription factors, including the nuclear factor κ B (NF- κ B) pathway, which instigates robust proinflammatory events. Activated NF- κ B triggers the production of an array of proinflammatory cytokines, e.g., tumor necrosis factor- α (TNF- α), which provokes DA neuronal death.^{3,7} Conversely, the glial cell line-derived neurotrophic factor (GDNF), a member of the transforming growth factor superfamily, is a potent trophic agent that promotes the survival and differentiation of DA neurons through the activation of the downstream PI3K/AKT pathway.⁸

Rotenone, a pesticide that inhibits mitochondrial complex I, has been widely used to induce several pathological changes and motor dysfunction of PD in rats. By virtue of its hydrophobicity, rotenone readily crosses the blood–brain barrier, and its chronic administration, particularly at lower doses, has been reported to incur selective degeneration of the nigrostriatal DA neurons. These deleterious actions are mediated via prompting mitochondrial oxidative stress, ATP depletion, and apoptosis.¹ Besides triggering DA neuronal degeneration, rotenone elicits LB formation and α -synuclein deposition. Generally, the rotenone-induced PD model meets the expectations of research studies on PD by recapitulating several anatomical, neurochemical, behavioral, and neuropathological features of the human condition.⁹

To date, the mainstay treatment strategies for PD focus on addressing the symptoms via enhancement of the dopaminergic effects without affecting the inevitable progressive neurodegeneration associated with the disease. Patients with PD continue to suffer a higher rate of mortality compared to the general population;¹ thus, the search for effective agents that can affect the disease progression merits attention. The newly developed sodium-glucose-linked transporter 2 (SGLT2) inhibitors are novel agents for the management of type 2 diabetes mellitus where they improve glycemic control with a minimum risk of hypoglycemia. The concept that the inhibition of renal SGLT2 results in glucosuria and diuresis without triggering hypoglycemia has been previously demonstrated by the pathogenesis of familial renal glucosuria. In that disorder, the genetic mutation of the SGLT2 gene has been manifested by glucosuria and diuresis, yet the blood glucose remains normal.^{10,11} Beyond their glucose-lowering ability, SGLT2 inhibitors have displayed marked reno- and cardioprotective features in diabetic patients and experimental animals.¹¹ In the context of neuroprotection, SGLT2 inhibitors have improved the cognitive function in diabetic (db/db) mice via abrogation of cerebral oxidative stress¹² and in high-fat diet (HFD)-fed mice through suppression of obesity-associated neuroinflammation.¹³

Dapagliflozin (DPG) is a selective/potent SGLT2 inhibitor that has demonstrated glucose-lowering effects in type 2 diabetes mellitus with a low risk of hypoglycemia.¹⁴ Even in normoglycemic animals, DPG has not lowered the blood glucose levels, as demonstrated in rats with coronary ligation-induced myocardial infarction.¹⁵ With regard to its neuroprotective features, DPG has attenuated the cognitive decline in HFD-fed rats,¹⁶ the seizure activity in a murine model of pentylenetetrazol (PTZ)-induced epilepsy,¹⁷ and the behavioral dysfunction in Huntington's disease in rats¹⁸ and improved the recognition memory in diabetic mice.¹⁹ In fact, the expression of SGLT2 in the mammalian central nervous system (CNS) has been demonstrated, where significant SGLT2 expression is characterized in endothelial cells of the blood–brain barrier (BBB), cerebellum, and hippocampus.²⁰

Notably, SGLT2 inhibitors, including DPG, are lipid-soluble drugs that can cross the BBB and access the CNS, especially under the inflammatory neurological conditions, including PD.^{20–22} In perspective, DPG attenuated the neuroinflammatory and apoptotic events in the brain striata of rats with Huntington's disease, confirming the ability of DPG to cross the BBB.¹⁸ Likewise, DPG ameliorated brain oxidative stress, mitochondrial dysfunction, apoptosis, inflammation, and hippocampal synaptic plasticity in the brain of rats with HFD-evoked cognitive decline.¹⁶ Despite these promising neuroprotective effects, the potential of DPG for the amelioration of rotenone-induced PD has not been previously examined. Thus, the present work aimed to investigate the potential of DPG to attenuate neuronal injury and motor dysfunction in rotenone-evoked PD model in rats. Given that hyperglycemia has been described to contribute to the neuronal degeneration in dopaminergic neurons,²³ normoglycemic animals were used in the present work to examine the possible neuroprotective role of DPG against PD, independent of its glucose-lowering effects.¹⁵ In fact, the use of normoglycemic animals for examining DPG's effects has been previously described in murine models of myocardial infarction¹⁵ and PTZ-induced epilepsy.¹⁷ Of note, no hypoglycemia or off-target gastrointestinal SGLT1 inhibition has been reported in normoglycemic rats^{15,24} at the low dose of DPG (1 mg/kg)/day by gavage) which was used in the present set of experiments.²⁵

RESULTS

Dapagliflozin Treatment Attenuates Motor Dysfunction and Improves Motor Performance without Lowering Blood Glucose Levels in Normoglycemic Rats with Rotenone-Induced PD. To explore the effect of DPG on the motor dysfunction triggered by rotenone, the motor performance was assessed by the open-field test, whereas the motor coordination was examined using the rotarod test. In the open-field test, rotenone significantly disturbed the motor activity of rats, as evidenced by decline of the total traveled distance (0.61-fold), mean speed (0.66-fold), line crossings (0.70-fold), and rearing frequency (0.64-fold), along with an obvious increase in the immobility time (1.8-fold), as compared to the control rats. In the rotarod test, rotenone suppressed the fall-off latency (0.58-fold; Figure 1A–G). Interestingly, DPG improved the motor performance as manifested by a prominent increase of the aforementioned motor parameters by 220%, 290%, 210%, and 210%, respectively, as compared to PD rats, together with a diminution of the immobility time by 54.5%. Moreover, DPG reverted the fall-off latency back to its normal values, signifying the enhanced motor coordination and balance. Track plots of animals in the open-field corroborated these findings (Figure 1F). Of note, the blood glucose levels were not significantly changed in rotenone or rotenone + DPG groups (Figure 1H). This is consistent with the previous literature that demonstrated no hypoglycemia in DPG-treated normoglycemic rats at the dose of 1 mg/kg, by gavage.²⁴ Consistent with the previous studies,^{15,24} we did not observe any gastrointestinal tract (GIT) disturbance, e.g., soft stool or diarrhea due to SGLT1 inhibition, confirming the selective SGLT2 inhibition at the used dose. Together, these findings indicate that DPG treatment elicited beneficial attenuation of the motor dysfunction and enhanced the motor coordination in rats with rotenone-induced PD.

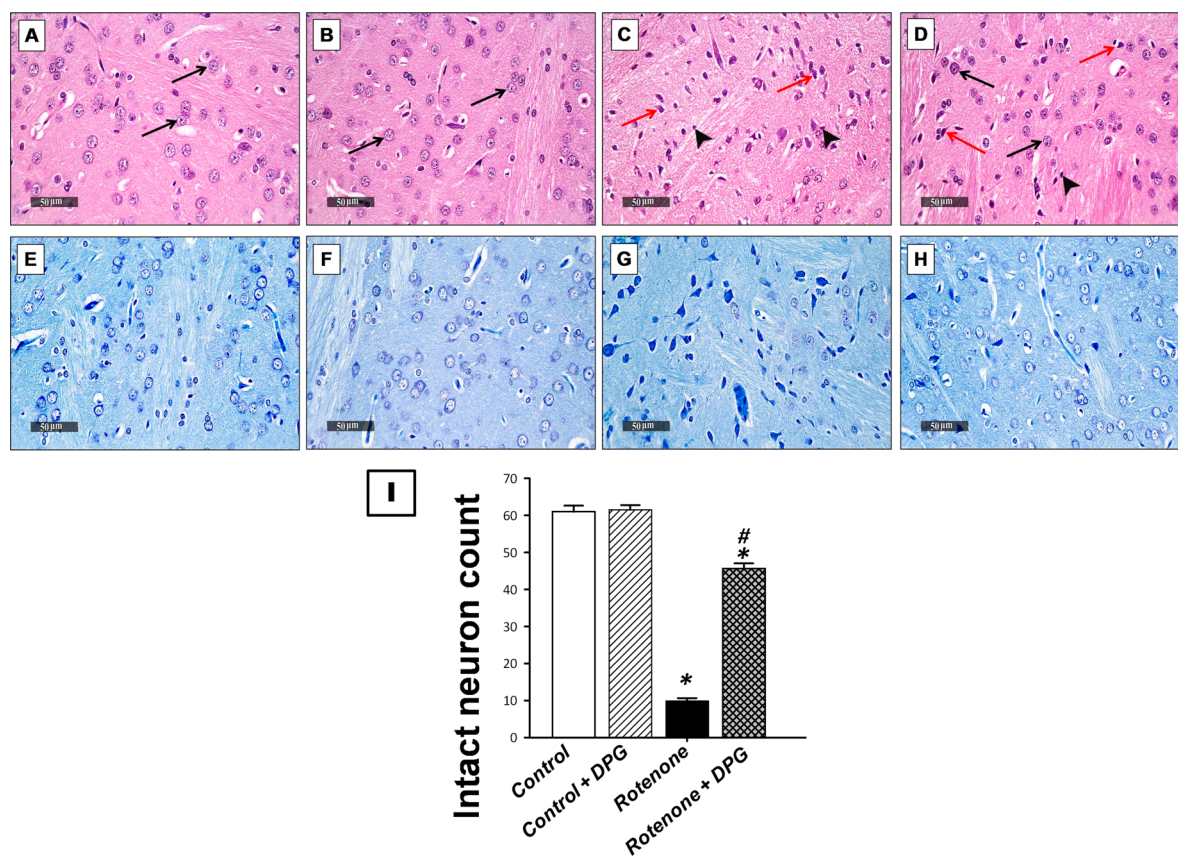


Figure 2. Dapagliflozin attenuates the neuronal degeneration and the histopathologic changes in the striata of rotenone-induced PD rats. (A–D) Histopathologic assessment using H&E stain at $\times 400$ magnification: (A) Representative photomicrograph of the striatum from the control group depicting normal striatal morphology showing well-organized neurons demonstrating intact perikaryons with large vesicular nuclei and prominent nucleoli (black arrows). Intact intercellular matrix with minimal glial-cell infiltrates is also evident. (B) Representative photomicrograph of the striatum from the control + DPG group showing normal striatal structure with normal neurons and no histopathologic alterations. (C) Representative photomicrograph of the striatum from the rotenone group showing wide diffuse areas of severe neuronal loss and damage with many degenerated, shrunken, and pyknotic neurons that lost their subcellular details (red arrows). The photomicrograph also demonstrates moderate perineuronal edema, moderate glial cell infiltrates (arrowheads), and moderate vacuolization of the intercellular matrix. (D) Representative photomicrograph of the striatum from rotenone + DPG group showing attenuation of the histologic alterations with many apparently intact neurons with preserved subcellular details (black arrows) and few scattered degenerative neurons (red arrows). An intact intercellular matrix was observed with minimal records of reactive glial-cell infiltrates (arrowheads). (E–H) Neuron visualization by Nissl staining at $\times 400$ magnification: (E, F) Representative photomicrographs of the striata from the control and control + DPG groups, respectively, showing intact neurons; (G) Representative photomicrograph of the striatum from the rotenone group showing a large proportion of degenerated neurons with pyknotic alterations; (H) Representative photomicrograph of the striatum from the rotenone + DPG group showing preserved neuronal integrity with a marked reduction of the degenerative neuronal records and higher records of intact neurons. (I) Assessment of the intact neuron count in the striatum of Nissl-stained sections. Data are expressed as the mean \pm SEM of number of intact neurons/field for six nonoverlapping fields/section; $n = 6$; * $P < 0.05$, statistical significance against the control group; # $P < 0.05$, statistical significance against the rotenone group; DPG, dapagliflozin.

Dapagliflozin Treatment Mitigates the Neuronal Degeneration and the Histopathologic Aberrations in the Striata of Rats with Rotenone-Induced PD. We next assessed whether DPG could protect the neuronal degeneration and the histopathologic changes in the striata of rats with rotenone-induced PD. Sections of the control group as well as the DPG-treated control exhibited an intact architecture of the striatum showing normal neurons with intact perikaryons and intact intercellular matrix with minimal glial cell infiltrates (Figure 2A,B,E,F). Conversely, the rotenone group demonstrated severe neuronal loss (Figure 2C,G,I), with many degenerated and pyknotic neurons and perineuronal edema accompanied by moderate glial cell infiltrates and intercellular matrix vacuolization. In line with the findings of the behavioral tests, DPG treatment attenuated these histopathologic

aberrations and counteracted the degeneration of neurons (Figure 2D,H,I).

Dapagliflozin Treatment Preserves the Dopaminergic Neurons, Lowers the Expression of α -Synuclein, and Enhances the Striatal Dopamine Levels in Rats with Rotenone-Induced PD. To characterize the molecular events linked to the rotenone-induced PD pathology and associated neuronal injury, the protein expression of tyrosine hydroxylase (TH), the rate-limiting enzyme of neuronal dopamine synthesis,¹ was investigated. Meanwhile, the mRNA expression of the neurotoxic α -synuclein, a hallmark protein aggregate that has been linked to PD pathology,¹ together with the neuronal dopamine levels were explored. Immunoblotting revealed that rotenone incurred a robust decline of TH expression (0.13-fold), as compared to the control group (Figure 3A,B). These data were corroborated by the

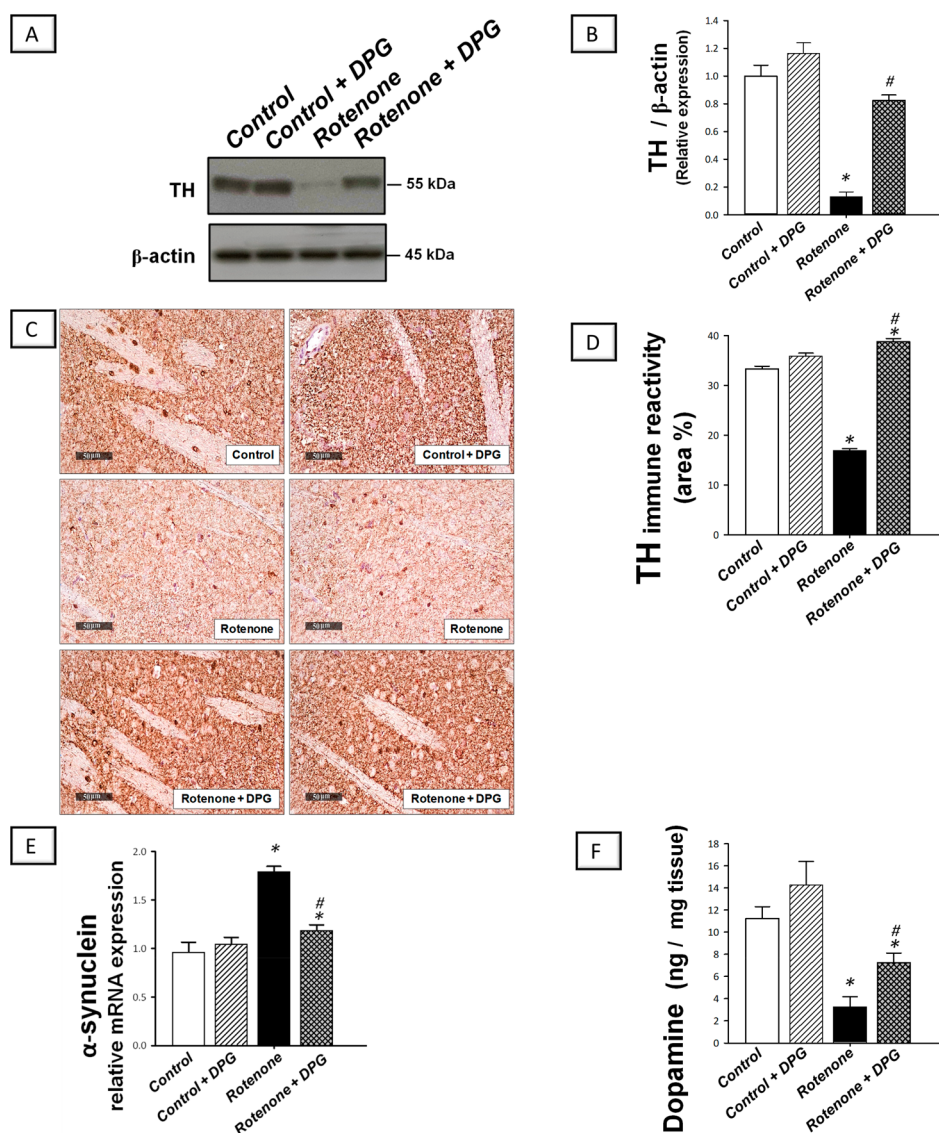


Figure 3. Dapagliflozin reverses rotenone-induced alterations of tyrosine hydroxylase (TH), α -synuclein, and dopamine levels in PD rats. (A) Protein expression of TH detected by immunoblotting. β -Actin was utilized as the loading control to prove equal protein loading. (B) TH relative protein expression. The values were extracted from at least three independent experiments (presented as the mean \pm SEM). (C) Representative photomicrographs of the immunohistochemical evaluation of TH protein expression (magnification $\times 400$). The control and control + DPG groups show intense TH staining, while the rotenone group shows a lower intensity of TH-immune reactivity. The rotenone + DPG group demonstrates reinstated TH protein expression. (D) Quantification of TH immunostaining in the striatum. Values are the mean \pm SEM of the area percentage of TH-immune staining to the total area of the microscopic field across six nonoverlapping fields/section; $n = 6$. (E) α -Synuclein relative mRNA expression detected by RT-qPCR and GAPDH was used as the housekeeping gene. The relative expression was calculated from the $2^{-\Delta\Delta CT}$ formula. (F) Dopamine levels. The values are the mean \pm SEM; $n = 6$; * $P < 0.05$, statistical significance against the control group; # $P < 0.05$, statistical significance against the rotenone group; DPG, dapagliflozin.

immunohistochemical detection of TH (Figure 3C,D). In the same context, the neuronal mRNA expression of the neurotoxic α -synuclein was increased (1.87-fold), ultimately provoking a decrease of the striatal dopamine levels (0.29-fold), as compared to the control group (Figure 3E and Figure 3F, respectively). The administration of DPG reversed these events, as manifested by the normalization of TH levels, suppression of α -synuclein expression by 34%, and enhancement of dopamine levels (221%), as compared to PD rats. Together, these findings reveal that DPG protects dopaminergic neurons and lowers the neurotoxic α -synuclein with consequent enrichment of the striatal dopamine levels, events

that are in line with the observed enhancement of the functional motor activity and coordination of rats.

Dapagliflozin Treatment Inhibits Neuronal Oxidative Changes and Restores DJ-1/Nrf2 Signaling in Rats with Rotenone-Induced PD. Given the fact that ROS-associated mitochondrial dysfunction/ATP depletion is a chief hallmark that mediates the selective loss of dopaminergic neurons in PD,³ we aimed to explore the antioxidant potential of DPG in the striata of PD rats by examining the lipid peroxides and the DJ-1 (PARK7)/Nrf2 signaling. Rotenone administration enhanced the striatal oxidative aberrations, as evidenced by increased lipid peroxide levels (4.3-fold), as compared to the control rats (Figure 4). Interestingly, DPG attenuated lipid

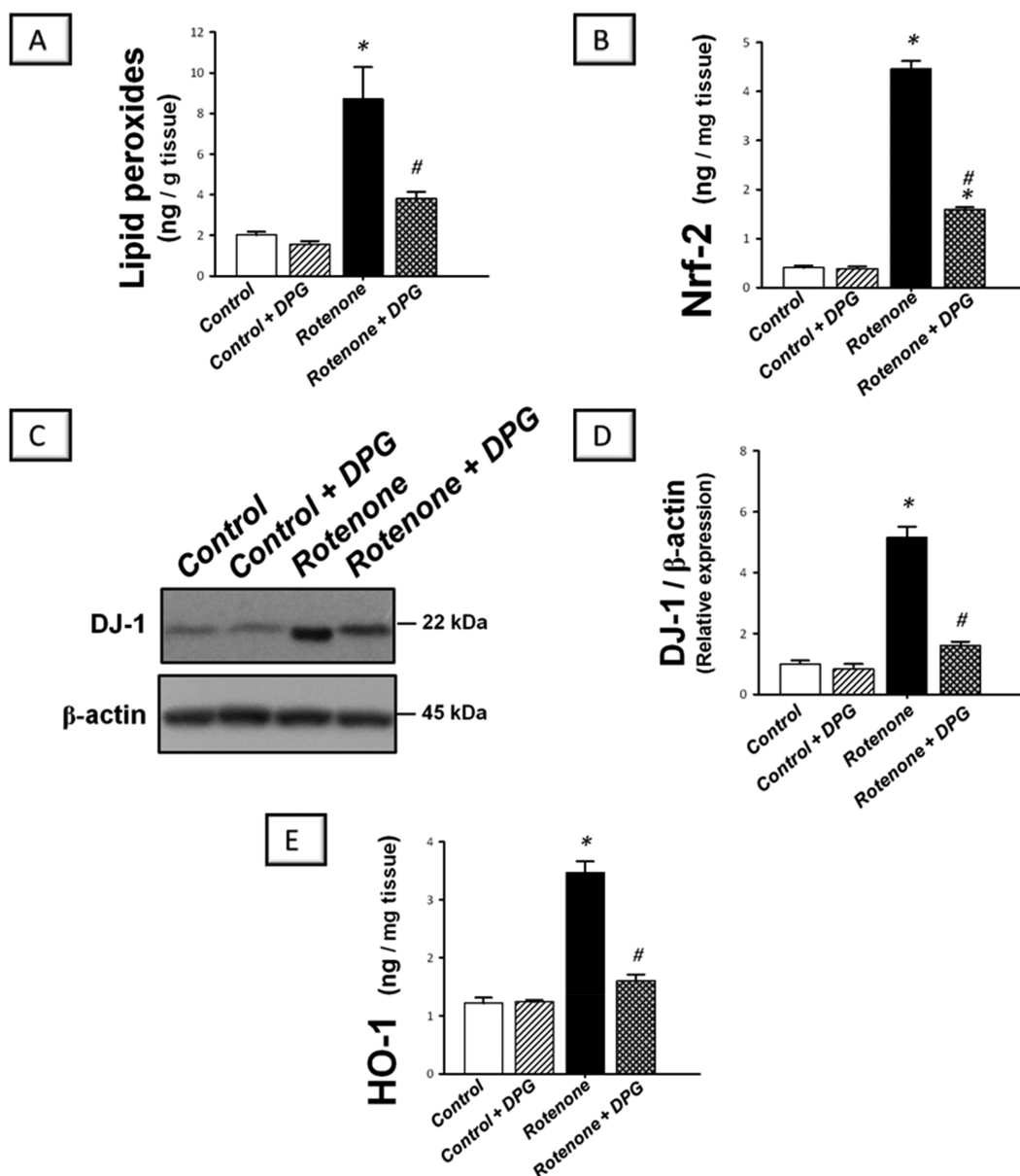


Figure 4. Dapagliflozin suppresses neuronal oxidative stress and restores the DJ-1/Nrf2 pathway in striata of rotenone-induced PD rats. (A) Lipid peroxides expressed as MDA. (B) Nuclear Nrf-2 protein expression. (C) Western blotting depicting the protein expression of DJ-1 protein. β -Actin served as the loading control. (D) DJ-1 relative protein expression. The values were extracted from at least three independent experiments (presented as the mean \pm SEM). (E) Heme oxygenase-1 (HO-1) levels. Values for lipid peroxides, Nrf2, and HO-1 are the mean \pm SEM; $n = 6$; * $P < 0.05$, statistical significance against the control group; # $P < 0.05$, statistical significance against the rotenone group; DPG, dapagliflozin.

peroxide levels by 56%, as compared to PD rats. To evaluate whether the observed antioxidant actions of DPG are related to the DJ-1/Nrf2 pathway, we investigated the expression of the upstream signal Nrf2 and its stabilizer protein DJ-1. Meanwhile, the transcriptional activity of Nrf2 was detected by measuring the levels of HO-1 protein. As displayed in Figure 4, rotenone increased the nuclear Nrf2 levels (11-fold) and the protein expression of DJ-1 (5.1-fold) and HO-1 (2.86-fold), as compared to the control rats. In line with the attenuation of lipid peroxides, DPG counteracted the changes of the DJ-1/Nrf2 pathway, as evidenced by lowering the protein expression of Nrf2, DJ-1, and HO-1 by 64.2%, 68.8%, and 53.8%, respectively, as compared to PD rats. These findings indicate that DPG's antioxidant actions are implicated in the

amelioration of rotenone-induced neuronal injury and PD pathology via the modulation of DJ-1/Nrf2 pathway.

Dapagliflozin Treatment Counteracts Neuronal Apoptotic Events and Augments GDNF and Its Downstream PI3K/AKT/GSK-3 β Signaling in the Striata of Rats with Rotenone-Induced PD. To determine the effects of DPG on the apoptotic events in rotenone-induced PD in rats, the mitochondrial energy markers ATP and ADP were assessed along with the protein expression of Bax and cleaved caspase-3. Rotenone triggered an impairment of the mitochondrial energy generation, as evidenced by decreased ATP (0.36-fold) and increased ADP levels (3.05-fold), as compared to the control rats (Figure 5). In the same regard, rotenone increased the protein expression of the proapoptotic Bax (2.52-fold) and cleaved caspase-3 (2.32-fold), as compared

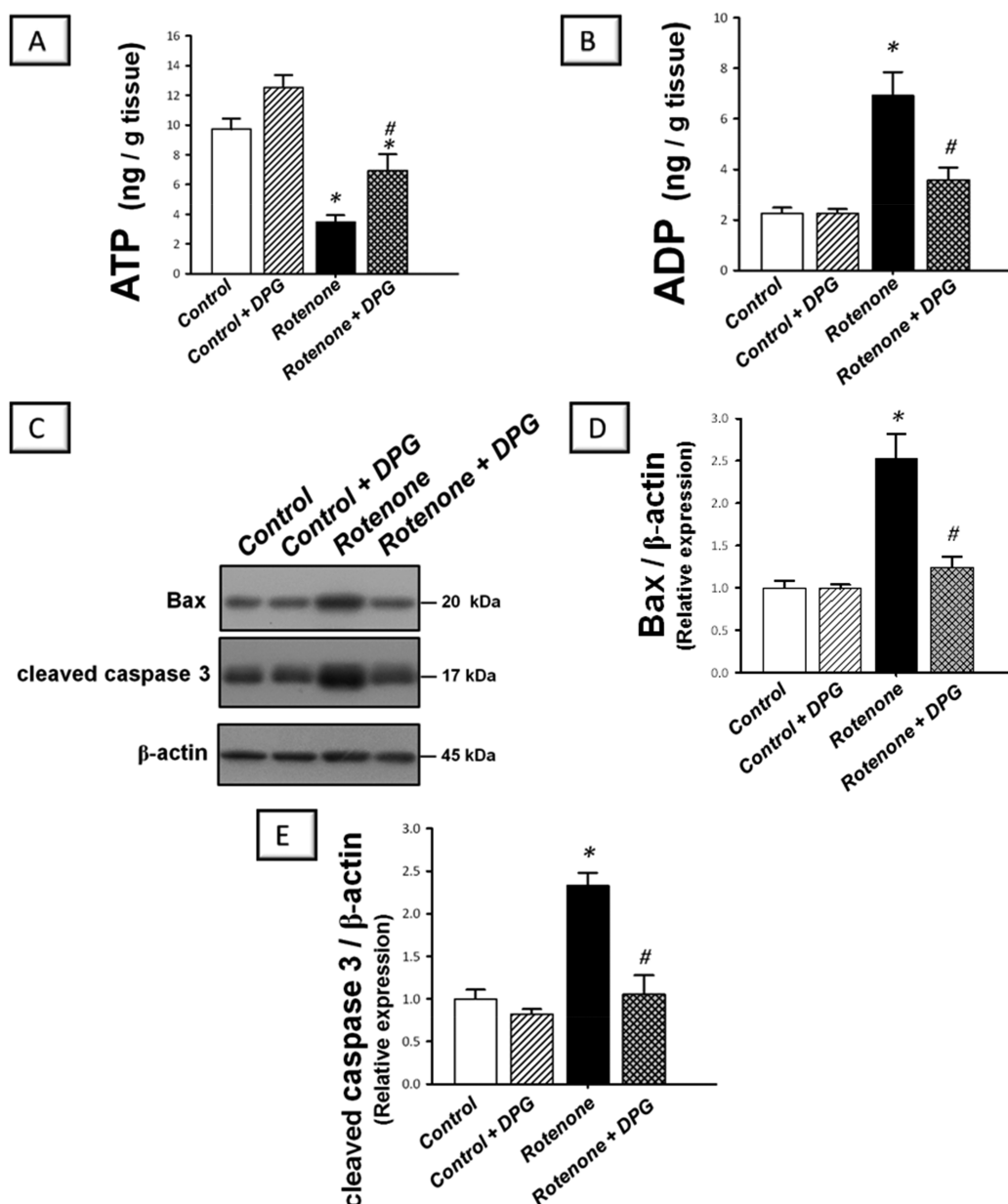


Figure 5. Dapagliflozin reverses the ATP depletion and neuronal apoptotic cell death in the striata of rotenone-induced PD rats. (A) ATP levels. (B) ADP levels. Values are the mean \pm SEM; $n = 6$. (C) Western blotting depicting the protein expression of the proapoptotic Bax (upper panel) and cleaved caspase-3 (middle panel). Equal protein loading was demonstrated using β -actin (lower panel). (D, E) Bax and cleaved caspase-3 relative protein expression, respectively. The values were extracted from at least three independent experiments (presented as the mean \pm SEM); * $P < 0.05$, statistical significance against the control group; # $P < 0.05$, statistical significance against the rotenone group; DPG, dapagliflozin.

to the control rats. Interestingly, DPG counteracted the disruption of energy generation by increasing the ATP production by 201% and it reversed the apoptotic aberrations by downregulating the expression of Bax and cleaved caspase-3 by 50.6% and 54.8%, respectively, as compared to PD rats.

To further explore the underlying antiapoptotic mechanisms, the striatal levels of GDNF and the signaling of its downstream PI3K/AKT/GSK-3 β pathway were detected. Rotenone diminished the striatal expression of GDNF (0.51-fold) and suppressed the PI3K/AKT/GSK-3 β pathway, as evidenced by downregulating the expression of PI3K (0.16-fold), p-AKT/AKT ratio (0.18-fold), and p-GSK-3 β Ser9/GSK-3 β ratio (0.36-fold), as compared to the control rats (Figure 6). In line with the attenuation of apoptosis, DPG reversed the above changes by increasing the expression of GDNF (173%) and

augmenting the PI3K/AKT/GSK-3 β pathway by increasing the expression of PI3K, p-AKT/AKT, and p-GSK-3 β (Ser9)/GSK-3 β by 480%, 528%, and 237%, respectively, as compared to PD rats. Overall, these findings reveal the marked antiapoptotic effects of DPG, which were mediated, at least partly, via upregulating the expression of GDNF and activating the PI3K/AKT/GSK-3 β pathway.

Dapagliflozin Treatment Suppresses the Neuroinflammation via Curbing of the Activation of the NF- κ B Pathway and Expression of TNF- α in the Striata of Rats with Rotenone-Induced PD. To explore the neuronal inflammatory events in PD rats, we investigated the activation of the NF- κ B pathway and the protein expression of the downstream effector TNF- α . The immunoblotting data demonstrated that rotenone incited NF- κ B activation as

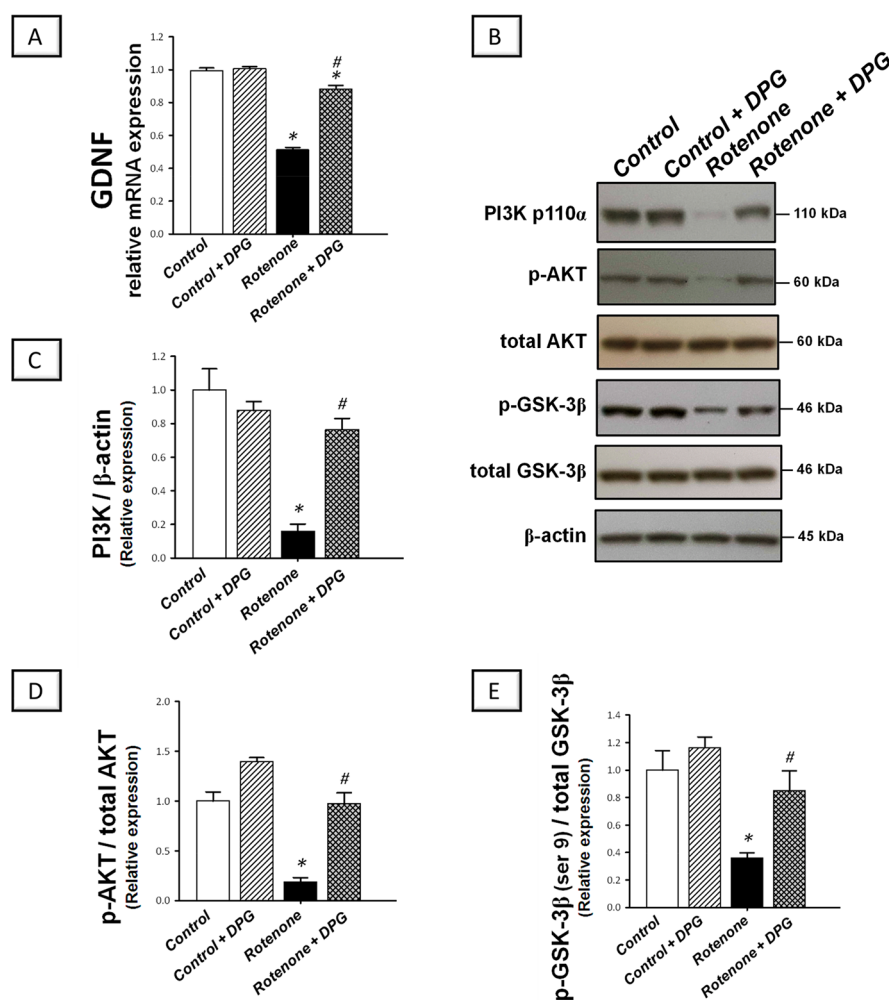


Figure 6. Dapagliflozin enhances the GDNF levels and PI3K/AKT/GSK-3 β signaling in the striata of rotenone-induced PD rats. (A) GDNF relative mRNA expression detected by RT-qPCR and GAPDH was used as the housekeeping gene. The relative expression was calculated from the $2^{-\Delta\Delta CT}$ formula. Values are the mean \pm SEM; $n = 6$. (B) Western blotting depicting the protein expression of the PI3K p110 α , p-AKT(Ser473), and total AKT (upper panel) alongside p-GSK-3 β (Ser9) and total GSK-3 β (lower panel). Equal protein loading was demonstrated using β -actin. (C) PI3K relative protein expression. (D) p-AKT(Ser473) relative protein expression. (E) p-GSK-3 β (Ser9) relative protein expression. The values were extracted from at least three independent experiments (presented as the mean \pm SEM); * $P < 0.05$, statistical significance against the control group; # $P < 0.05$, statistical significance against the rotenone group; DPG, dapagliflozin.

evidenced by increased protein expression of activated NF- κ Bp65 (4.2-fold) and its phosphorylated form (p-NF- κ Bp65; 6.3-fold) together with increased expression of TNF- α (3.34-fold), as compared to the control rats (Figure 7). These findings were corroborated by the immunohistochemical detection of activated NF- κ Bp65 that revealed an extensive expression in the striata of PD rats (8.08-fold), as compared to the control rats (Figure 7D,E). DPG counteracted these alterations via downregulating the expression of NF- κ Bp65 and p-NF- κ Bp65 by 66.9% and 73%, respectively, and TNF- α by 47.9%, as compared to PD rats. Meanwhile, DPG downregulated the immunohistochemical staining of NF- κ Bp65 by 67.7%, as compared to PD rats. These findings reinforce the notion that DPG's suppression of neuronal inflammation is implicated in the attenuation of neuronal injury and rotenone-induced PD pathology.

DISCUSSION

Current treatment strategies for PD are directed to alleviate the symptomatic features of the disease without modifying its

underlying multifactorial pathology.³ Thus, the quest for therapeutic interventions with multipronged effects on PD progression has been envisioned as an efficient strategy. The present study demonstrates, for the first time, the beneficial effects of DPG against rotenone-induced neuronal injury and PD motor dysfunction in rats. Interestingly, DPG attenuated the PD motor deficits, histopathologic aberrations, and α -synuclein expression and preserved the striatal dopaminergic neurons. Mechanistically, DPG inhibited neuronal ROS/oxidative changes with consequent restoration of the DJ-1/Nrf2 pathway. These events primed the counteraction of neuronal apoptosis and boosting of the GDNF levels and associated activation of the PI3K/AKT/GSK-3 β pathway. In tandem, DPG suppressed the neuroinflammation via inhibition of the NF- κ B pathway (Figure 8).

The current data demonstrated enhanced oxidative stress in the striata of PD rats marked with increased lipid peroxide levels and increased levels of DJ-1, nuclear Nrf2, and the downstream signal HO-1. These findings are consistent with previous reports^{26–29} that characterized an upregulated DJ-1

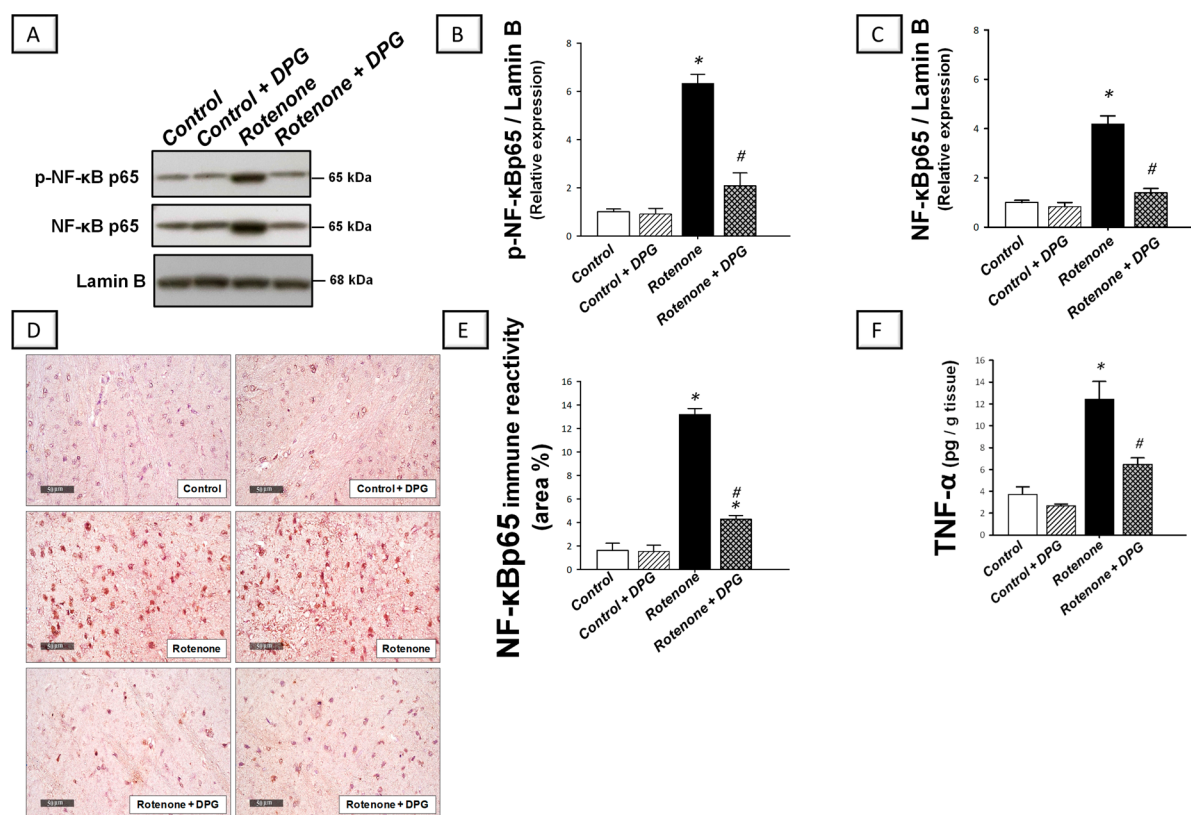


Figure 7. Dapagliflozin suppresses the activation of the NF- κ B pathway and TNF- α level in the striata of rotenone-induced PD rats. (A) Western blotting describing the expression of the phospho-NF- κ Bp65 and the nuclear NF- κ Bp65. Lamin B was utilized as loading control. (B, C) Phospho-NF- κ Bp65 and nuclear NF- κ Bp65 relative protein expression, respectively. The values were extracted from at least three independent experiments (presented as the mean \pm SEM). (D) Staining of NF- κ Bp65 protein expression detected by immunohistochemistry (the representative photomicrographs are shown at 400 \times magnification). The control and control + DPG groups show minimal staining, while the rotenone group shows strong positive staining. The rotenone + DPG group demonstrates attenuated expression of NF- κ Bp65 protein. (E) NF- κ Bp65 immunostaining quantification in the striatum. Values are the mean \pm SEM of area percentage of NF- κ Bp65 immunostaining to the total area of the microscopic field across six nonoverlapping fields/section; $n = 6$. (F) Tumor necrosis factor- α (TNF- α) levels. Values are the mean \pm SEM; $n = 6$; * $P < 0.05$, statistical significance against the control group; # $P < 0.05$, statistical significance against the rotenone group; DPG, dapagliflozin.

expression in response to rotenone treatment *in vivo* and *in vitro*. In fact, upregulation^{28,29} and downregulation^{30,31} of the Nrf2/HO-1 pathway have been described in the pathogenesis of rotenone-induced PD model. When subjected to oxidative stress, DJ-1 itself is oxidized at cysteine residues which enables it to scavenge ROS.²⁸ Virtually, oxidative stress and mitochondrial dysfunction play a pivotal role in the pathogenesis of PD in human patients and experimental models.^{29,32} DJ-1 is a redox-sensitive protein that protects neurons against oxidative stress and cell death. Mutations of DJ-1 have been associated with an early onset of PD symptoms, due to the neurodegeneration of nigrostriatal dopaminergic neurons. At the molecular level, DJ-1 serves as a stabilizer of Nrf2 by disrupting the Keap1/Nrf2 complex and/or preventing the interaction of Nrf2 with Keap1.³³ Hence, it minimizes Nrf2 ubiquitination and 26S proteasomal degradation and thus enhances its transactivation.²⁷ Several lines of evidence have characterized Nrf2 as a key interception point for the crosstalk among diverse cytoprotective, antioxidant, and anti-inflammatory pathways.²⁷ Nrf2 and its downstream signal HO-1 act as sensors of the pro-oxidant stressors which are induced as a compensatory mechanism to halt the deleterious effects of ROS and free radicals.³⁴ Despite the observed upregulation of Nrf2 in the rotenone-treated rat striata, oxidative stress was obviously detected, as evidenced by increased lipid peroxides.

This can be attributed to the rotenone-induced lowering of the inactive GSK-3 β (Ser9), an event that has been described to interfere with Nrf2 antioxidant action, likely via its nuclear exclusion, thus impeding its transactivating function.³⁵ In fact, Nrf2 ablation has been reported to result in exaggerated oxidative stress that drives activation of the redox-responsive NF- κ B and linked proinflammatory events, thereby pointing to the interplay between Nrf2 and NF- κ B cascades.³⁴ In the same context, the crosstalk between Nrf2/HO-1 and PI3K/AKT pathway advocates that restraining Nrf2 activity negatively affects the PI3K/AKT pathway, culminating in neuronal proapoptotic events.³⁶ Conversely, AKT has been reported to be engaged in the Nrf2 nuclear localization, confirming the mutual interaction between Nrf2 and AKT.²⁷

Interestingly, DPG suppressed the oxidative changes and restored the levels of DJ-1, Nrf2, and HO-1, pointing to its significant antioxidant effects for attenuation of PD pathology via the modulation of DJ-1/Nrf2 signaling. In fact, DPG has demonstrated marked antioxidant effects in obesity-induced cognitive decline¹² and myocardial infarction via suppression of ROS.¹⁵ Given the fact that ROS are the main triggers for upregulation of DJ-1/Nrf2, it may be straightforward to understand that the observed DPG-induced restoration of Nrf2/HO-1 pathway is secondary to the lowering of ROS and the associated neuronal oxidative stress.³⁴ In fact, the

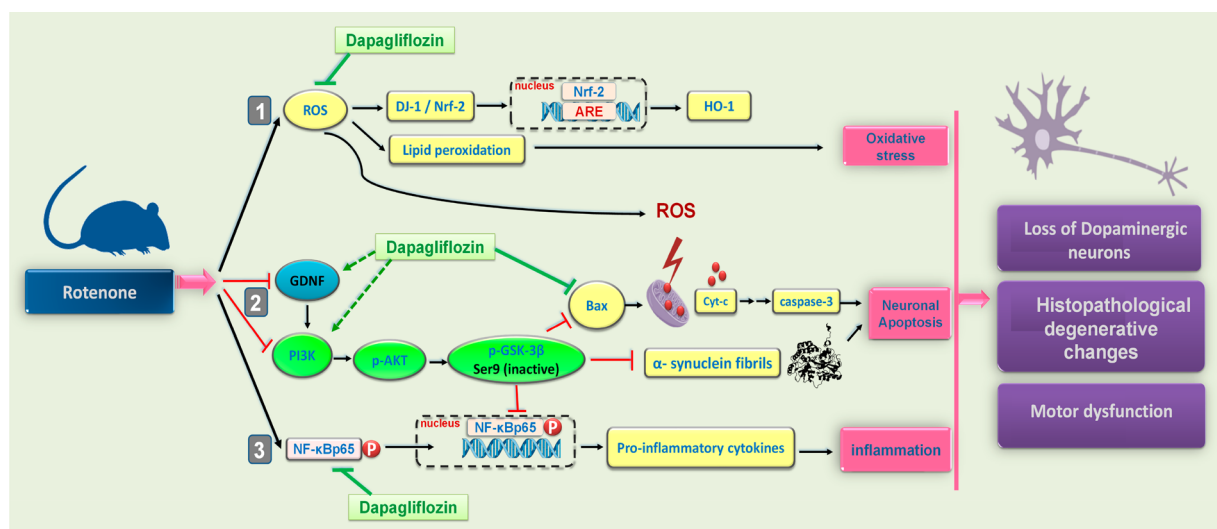


Figure 8. Summary of the underlying mechanisms for dapagliflozin's amelioration of rotenone-induced neuronal injury and PD pathogenesis. According to the current study findings, dapagliflozin, a selective SGLT2 inhibitor, attenuated the neuronal injury through the following actions: (1) curbing the ROS/oxidative aberrations, an event that resulted in the restoration of the DJ-1/Nrf2 pathway and associated transactivation of antioxidant response element (ARE) genes encoding HO-1 back to its normal levels. The attenuation of neuronal oxidative stress and ROS production primed the counteraction of ROS-dependent apoptosis and neuroinflammation, as illustrated in steps 2 and 3. (2) Dampening the apoptotic machinery and boosting the GDNF and associated activation of the prosurvival PI3K/AKT pathway with consequent inactivation of GSK-3 β (via Ser9 phosphorylation). (3) Suppression of the NF- κ B pathway that resulted in lowered proinflammatory cytokine production (e.g., TNF- α) and neuroinflammation. Together, these events ultimately lowered the expression of the neurotoxic α -synuclein in the dopaminergic neurons, thereby minimizing their loss. Black solid arrow, activate; red blunt arrow, inhibit; green dotted arrow, activating effect of dapagliflozin; green blunt arrow, inhibitory effect of dapagliflozin.

mitigation of neuronal oxidative stress by DPG accentuates the crucial role of its antioxidant features for ameliorating PD neurodegeneration and is likely due to the observed DPG-induced inactivation of GSK-3 β (via its phosphorylation at Ser9) and suppression of the NF- κ B pathway. In this context, the observed inactivation of GSK-3 β by DPG is plausibly a key player in the suppression of neuronal oxidative stress, since GSK-3 β blockade has been proven to alleviate oxidative damage in several neuronal models.^{3,7} Meanwhile, the observed DPG-evoked suppression of the NF- κ B pathway also contributes to curtailing neuronal oxidative stress elicited by the pro-oxidant features of NF- κ B in PD models.³⁷ Interestingly, previous reports have revealed that substantia nigra dopaminergic neurons can be protected via the Nrf2 pathway and p62-associated autophagy activation.³⁸ In fact, autophagy has been reported to exert antioxidant actions in PD via the removal of oxidized/dysfunctional cellular organelles and proteins.³⁹ Moreover, the interventions that restore the balance between autophagy and apoptosis have been proven effective for combating the neuropathological changes in rotenone-induced PD model.^{39,40} In this context, dopaminergic neuron loss in the substantia nigra has been halted via enhancing Ser70 phosphorylation of Bcl-2 and the subsequently increased autophagy/apoptosis ratio.⁴⁰ Notably, additional studies exploring the detailed effects of dapagliflozin on autophagy and associated mechanisms are requested.

The present findings further demonstrated a disrupted mitochondrial ATP production and enhanced apoptosis in the striata of rotenone-induced PD, as evidenced by upregulated expression of the proapoptotic Bax and cleaved caspase-3. These apoptotic events are likely driven by the exaggerated neuronal oxidative stress and proinflammatory reactions.²⁶ In fact, excessive mitochondrial ROS generation impairs the respiratory chain function and ATP generation, events that

play a pivotal role in the pathogenesis of neurodegenerative diseases, such as PD since adequate energy supply to the CNS is crucial for neuronal survival and excitability.^{3,41} In the context of apoptotic events, an enhanced expression of the cleaved caspase-3 has been described in post-mortem PD patients and rodent models of PD.^{42,43} Meanwhile, the current data revealed that rotenone lowered the levels of the neurotrophic factor GDNF and disrupted its downstream PI3K/AKT/GSK-3 β signaling in the striata of rats. In the context of apoptosis, the dysregulation of PI3K/AKT/GSK-3 β pathway has been reported to play a crucial role in PD pathology.^{3,7} The PI3K/AKT pathway has been reported to inactivate the proapoptotic/proinflammatory GSK-3 β via its Ser9 phosphorylation. The dysregulation of PI3K/AKT signaling has been described in post-mortem dopaminergic neurons of PD patients where low p-AKT/AKT levels were detected.⁶ In this regard, α -synuclein has been suggested as a causative signal for activating the proapoptotic/proinflammatory GSK-3 β (via its Tyr216 phosphorylation) in the striatum of post-mortem PD patients and transgenic PD mice.^{3,44} In addition, the overexpression of active GSK-3 β in mitochondria has been reported to disrupt ATP generation, enhance oxidative stress, and exacerbate the apoptotic effects of rotenone via promoting of cytochrome *c* release and caspase-3 activation.⁴⁵

Interestingly, DPG hampered the apoptotic machinery, upregulated the upstream GDNF, and activated the prosurvival PI3K/AKT pathway with consequent inactivation of GSK-3 β (via Ser9 phosphorylation). These pleiotropic antiapoptotic actions of DPG are in line with its reported suppression of neuronal apoptosis in obesity-induced cognitive decline via diminishing Bax levels and rectifying mitochondrial dysfunction.¹² The multipronged antiapoptotic actions of DPG are mainly ascribed to the observed boosting of the neurotrophic

Table 1. Experimental Design and Study Groups^a

group	description
Group I (control)	Group I (control) received 11 subcutaneous injections of 1% (v/v) DMSO (0.2 mL/kg) on an alternate-day basis corresponding to rotenone administration days for groups III and IV, in addition to normal saline (5 mL/kg) by gavage daily for 3 weeks starting from the first day to serve as the control group.
Group II (control + DPG)	Group II (control + DPG) received 11 subcutaneous injections of 1% DMSO (0.2 mL/kg) on an alternate-day basis corresponding to rotenone administration days for groups III and IV, in addition to DPG suspended in normal saline (1 (mg/kg)/day; 5 mL/kg) by gavage ¹⁶ for 3 weeks starting from the first day to serve as the drug control group.
Group III (rotenone)	Group III (rotenone) received 11 subcutaneous injections of rotenone (1.5 mg/kg; 0.2 mL/kg) dissolved in 1% DMSO every other day, ⁵⁰ in addition to normal saline (5 mL/kg) by gavage daily for 3 weeks starting from the first day.
Group IV (rotenone + DPG)	Group IV (rotenone + DPG) received 11 subcutaneous injections of rotenone (1.5 mg/kg; 0.2 mL/kg) dissolved in 1% DMSO every other day, in addition to a daily dose of DPG (1 mg/kg; 5 mL/kg) by gavage for 3 weeks, starting from the first day, 1 h before the rotenone injection on the days of rotenone administration.

^aDMSO, dimethyl sulfoxide; DPG, dapagliflozin.

factor GDNF and the subsequent activation of the PI3K/AKT pathway. Conceptually, therapeutic interventions that activate PD neuronal PI3K/AKT pathway have been reported to afford marked neuroprotection in several neurodegenerative models, including PD.³ A mutual interplay has been described between neurotrophic factors, e.g., GDNF and AKT where some protective actions of GDNF are achieved through the AKT signaling.³ Conversely, AKT activation has been reported to upregulate the expression of GDNF.⁴⁶ The current observation that DPG inactivated GSK-3 β , via its Ser9 phosphorylation, may also point to its effective role for the abrogation of α -synuclein-induced neurotoxicity and cell death.^{3,46} Several *in vitro* as well as *in vivo* studies confirmed that the blockade of GSK-3 β is an effective tool against dopaminergic neurodegeneration via multipronged moderation of several pathogenic targets, e.g., neuronal oxidative stress, inflammatory signals, along with mitochondrial dysfunction and associated apoptosis.³

The current data revealed that PD rats demonstrated marked neuronal inflammation evidenced by the activation of NF- κ B signaling/upregulation of its downstream effector TNF- α , findings that are consistent with previous studies.^{5,37} Notably, TNF- α can bind to the TNF receptor (TNFR), culminating in NF- κ B pathway activation.^{37,47} Ample evidence has revealed that α -synuclein drives persistent inflammatory responses and glial cell activation with consequent degeneration of the dopaminergic neurons in PD patients and animal models.^{5,37} In this regard, NF- κ B is a key proinflammatory pathway that provokes neuroinflammation in response to excessive ROS, proinflammatory cytokines, and GSK-3 β activation.^{37,47} It has been reported that p-GSK-3 β (Tyr216) triggers the activation of NF- κ B signaling and associated transcription of several proinflammatory signals via I κ B kinase (IKK)-induced phosphorylation and degradation of the I κ B inhibitory subunit.³ Of note, the glial-cell-driven proinflammatory events may contribute to neuronal oxidative damage via overshooting of the neurotoxic ROS and prostaglandins, which ultimately elicit neuronal death.⁴⁸

Remarkably, DPG elicited significant anti-inflammatory actions via curbing neuronal NF- κ B activation and its downstream signal, TNF- α . These anti-inflammatory effects are in accord with previous studies.¹⁵ The observed suppression of GSK-3 β (via Ser9 phosphorylation) may contribute to the extenuation of neuronal inflammation. This can be conceived from the fact that the GSK-3 β inhibitor, lithium chloride, has been reported to repress proinflammatory signals, including TNF- α , and promote the production of the anti-inflammatory IL-10 in PD models.^{3,49} GSK-3 β inhibition has also been proven to be effective against 6-OHDA-induced

neurotoxicity via the blockade of microglial activation.^{7,49} The observed DPG-induced activation of the upstream PI3K/AKT signaling may also participate in the suppression of neuronal inflammation since the AKT kinase is responsible for Ser9 phosphorylation/inactivation of GSK-3 β which ultimately suppresses the proinflammatory NF- κ B signaling.³

CONCLUSION

For the first time, the current findings reveal that dapagliflozin, independent of its glucose-lowering effects, has demonstrated neuroprotective actions against rotenone-evoked neuronal injury and PD motor dysfunction in rats. These beneficial effects were chiefly elicited via suppression of neuronal oxidative stress and associated restoration of the DJ-1/Nrf2 pathway. The attenuation of ROS production primed the counteraction of apoptosis, boosting GDNF and associated PI3K/AKT/GSK-3 β signaling alongside the suppression of NF- κ B-linked neuroinflammation. Together, the current data recommend that dapagliflozin may offer a promising intervention for mitigating the neuropathological aberrations of PD, which may be useful in type II diabetes mellitus patients with coexisting PD. Prospective studies are warranted to gain further insights into the exact molecular mechanisms and signaling networks implicated in dapagliflozin's neuroprotective actions, in particular, the autophagy-related mechanisms. Moreover, it would be advisable to test the potential efficacy of dapagliflozin for combating the manifestations of PD in the clinical setting, especially in type II diabetic patients with coexisting PD.

MATERIALS AND METHODS

Drugs and Chemicals. Dapagliflozin was obtained from AstraZeneca (Cairo, Egypt). Rotenone and dimethyl sulfoxide (DMSO) were purchased from Sigma-Aldrich Chemical Co. (St. Louis, MO, USA). All other chemicals were of pure analytical grade.

Animals. The present study was conducted with adult male Wistar rats, weighing 230 \pm 20 g, which were obtained from the laboratory animal farm of the Egyptian Organization for Biological Products and Vaccines (VACSERA), Cairo, Egypt. The animals were accommodated in the animal facility of Faculty of Pharmacy, Cairo University, under controlled environmental conditions, including a temperature of 25 \pm 2 $^{\circ}$ C, 60 \pm 10% humidity, and a 12/12 h light/dark cycle, and were allowed free access to standard rodent chow diet and water.

Ethical Approval. All animal handling and testing procedures abided by the regulations set in the Guide for the Care and Use of Laboratory Animals issued by the U.S. National Institutes of Health (NIH Publication No. 85-23, revised 1996) and were approved by the Research Ethics Committee of Faculty of Pharmacy, Cairo University (REC-FOPCU, Permit Number BC 2717).

Experimental Design. The rats were allowed to acclimatize for 1 week before starting the study which spanned over a total period of 21

Table 2. List of Primer Sequences Used in the Real-Time qPCR Analysis^a

gene	primer sequence	accession number
α -synuclein	F: 5'-CCCTAGCAGTGAGGCTTATGA-3' R: 5'-CACAGCACATCATTCTTCTTAG-3'	NM_019169.2
GDNF	F: 5'-TAGAAGGCTGGTGTAGTGACAAAGTA-3' R: 5'-TCATCTAAAAACGACAGGTCATCATC-3'	NM_019139.1
GAPDH	F: 5'-TTGGTATCGTGAAGGACTCA-3' R: 5'-TGTCATCATATTTGGCAGGTTT-3'	NM_017008.4

^aGDNF, glial-cell-line-derived neurotrophic factor; GAPDH, glyceraldehyde 3-phosphate dehydrogenase.

days. The rats were randomly assigned into four groups ($n = 18$ each), as described in Table 1.

The dose of DPG was selected based on previous reports in the literature that demonstrated the alleviation of cognitive decline in HFD-fed rats and PTZ-induced epilepsy.^{16,17} Moreover, on the basis of the human equivalent dose (HED) calculation method,⁵¹ the selected dose for rats (1 mg/kg/day, po) is quite consistent with the commonly used dose of DPG in the clinical practice for humans. The selected dose of rotenone is in harmony with previous reports^{26,52} that characterized the 1.5 mg/kg dose of rotenone as a reliable dose for induction of consistent PD manifestations in rats. Herein, male rats were used to conduct the current experimental protocol since male rats have been reported to be more sensitive to the induction of rotenone-induced Parkinson's manifestations and associated histopathological findings than female rats.⁵³

Blood Glucose Assessment. Twenty-four hours after the last rotenone dose, blood samples were obtained through tail vein puncture and were analyzed by a portable glucometer (AccuCheck Performa, Roche Diagnostics, USA).

Behavioral Assessment. Following blood glucose measurement, all rats were tested for motor perturbations using the open-field and rotarod tests, as follows:

Open-Field Test. The open-field test was carried out to examine the spontaneous locomotor activity of rats. The test was carried out using a square wooden box (80 cm \times 80 cm \times 40 cm) with red walls and a white smooth polished floor divided by black lines into 16 equal squares 4 \times 4. The test was performed under dim white light in a quiet room, and an overhead camera was used to monitor the animals. Each rat was gently placed in the center of the open-field and was allowed to freely explore the area for 5 min. The floor and walls were thoroughly wiped after each tested animal to eliminate possible bias due to odors left by previous rats.⁵⁴ Total distance traveled, mean speed, line crossings, rearing frequency, and immobility time were recorded using ANY-maze behavioral tracking software (Stoelting, CO, USA).

Rotarod Test. Rats were screened for motor coordination and balance using rotarod apparatus (120 cm long and 3 cm in diameter which rotates at a constant speed of 20 rpm). Before experimental procedures, rats were habituated to maintain posture on the rotarod by three training sessions, 5 min each, on 3 consecutive days. After accomplishing the open-field test, rats were allowed to move over the rotarod and the latency until falling was recorded using a cutoff limit of 300 s.⁵⁵

Brain Tissue Processing. After the evaluation of motor performance, rats in each group were split into three sets and then were sacrificed by decapitation under light anesthesia. Immediately after decapitation, brains were rapidly dissected and washed with ice-cold saline. In the first set ($n = 6$ per group), brains were instantly fixed in 10% (v/v) neutral buffered formalin for 72 h to perform histopathologic and immunohistochemical examinations. In the second and third sets, both striata were excised from each brain under ice-cold conditions and then stored at -80 °C for biochemical and molecular analyses. In the second set ($n = 6$ per group), the striata were homogenized in ice-cold phosphate buffered saline (PBS), and the striatal homogenate was used for enzyme-linked immunosorbent assay (ELISA) analyses. In the third set ($n = 6$ per group), striatal tissues were used for gene expression and Western blot analyses.

Enzyme-Linked Immunosorbent Assay of Striatal Dopamine, ADP, ATP, MDA, TNF- α , Nrf2, and HO-1 Levels. The striatal homogenate was used for the determination of dopamine, ADP, ATP, lipid peroxides (malondialdehyde, MDA), tumor necrosis factor- α (TNF- α), nuclear factor erythroid 2-related factor (Nrf2), and heme oxygenase-1 (HO-1) levels by enzyme-linked immunosorbent assay (ELISA) technique. The dopamine neurotransmitter and the proinflammatory TNF- α were quantified using ELISA kits (catalog numbers CSB-E08660r and CSB-E11987r, respectively) purchased from Cusabio (Wuhan, China). The levels of the energy markers, ADP and ATP were determined using ELISA kits (catalog numbers MBS744390 and MBS723034, respectively) purchased from MyBioSource (San Diego, CA, USA). The assay kit for ADP is specific for ADP without cross-reacting with other ADP analogues, and it offers a sensitivity of 0.1 ng/mL as the minimum limit of detection. Likewise, the ATP ELISA kit is selective for ATP without a cross-reaction with ATP analogues and shows a 1 ng/mL as the minimum level of sensitivity. The striatal MDA content was assessed, as an index of lipid peroxidation, by an ELISA kit (catalog number LS-F28018) obtained from LifeSpan BioSciences (Seattle, WA, USA). Assay of the redox-sensitive transcription factor, Nrf2 was carried out in the striatal nuclear extract using an ELISA kit (catalog number 600590) from Cayman Chemical (MI, USA). The nuclear fraction was isolated from the striatal tissue homogenate using a nuclear extraction kit (catalog number 10009277) provided by Cayman Chemical (MI, USA). The Nrf2-regulated downstream HO-1 protein expression was assayed using an ELISA kit (catalog number MK124) procured from Takara Bio Inc. (Shiga, Japan). The ADP, ATP, and MDA ELISA kits applied the competitive enzyme immunoassay technique. Dopamine, TNF- α , and HO-1 assays employed the quantitative sandwich enzyme immunoassay technique. The Nrf2 ELISA technique detected the specific DNA binding activity of the transcription factor in the nuclear extract by capturing the transcription factor using an immobilized specific double-stranded DNA (dsDNA) sequence containing the Nrf2 response element. The unknown concentrations were determined by interpolation from the corresponding calibration curves relating the generated color intensities to known standard concentrations. The results are expressed as ng/mg tissue for dopamine, Nrf2, and HO-1 levels, ng/g tissue for ADP, ATP and MDA levels, and pg/g tissue for TNF- α content. All procedures were carried out in accordance with the manufacturers' guidelines.

Gene Expression Analysis of Striatal α -Synuclein and GDNF. The mRNA expression levels of α -synuclein and the glial-cell-line-derived neurotrophic factor (GDNF) were analyzed in the brain striatum by qRT-PCR.⁵⁶ Total RNA was isolated from striatal tissues using the standard TRIzol reagent extraction method (catalog number 15596-026, Invitrogen, Germany) according to the manufacturer's instructions. The purity of the extracted RNA was assessed by the 260/280 nm ratio, and its integrity was confirmed by ethidium bromide stain analysis of 28S and 18S bands by formaldehyde-containing agarose gel electrophoresis. Thereafter, the isolated RNA was reverse transcribed into complementary DNA (cDNA) using a RevertAid first strand cDNA synthesis kit (MBI Fermentas, Germany), in compliance with the manufacturer's protocol. To evaluate the expression of α -synuclein and GDNF genes, qRT-PCR was carried out using SYBR Premix Ex Taq II (Takara, Japan) in accordance with the manufacturer's guidelines. In

brief, qRT-PCR reactions were conducted in 25 μ L of reaction mixtures containing 5 μ L of cDNA, 12.5 μ L of SYBR Premix Ex TaqII reagent, 0.5 μ L of 0.2 μ M of each primer, and 6.5 μ L of RNase-free water. The primer sequences used are listed in Table 2. The PCR protocol comprised 10 min at 95 $^{\circ}$ C for initial DNA polymerase activation, followed by 40 cycles of denaturation at 95 $^{\circ}$ C for 15 s, and annealing/extension at 60 $^{\circ}$ C for 60 s. The relative expression of the target genes was calculated by the comparative cycle threshold (CT) method using the $2^{-\Delta\Delta CT}$ formula, where glyceraldehyde 3-phosphate dehydrogenase (GAPDH) was used as a housekeeping gene.

Western Blot Analysis of Striatal TH, p-NF- κ Bp65/NF- κ Bp65, DJ-1, Bax, Cleaved Caspase-3, PI3K, p-AKT/AKT, and p-GSK-3 β (Ser9)/GSK-3 β Protein Expression. The protein extraction process for the whole tissue lysate of the striatum and the Western blotting were carried out as previously described.⁵⁷ In addition, the nuclear fraction lysate was obtained with the aid of Cayman nuclear extraction kit (catalog number 10009277; Ann Arbor, MI, USA). Equal amounts of protein lysates were resolved by SDS-PAGE and were transferred to PVDF membranes. After blocking with 5% bovine serum albumin (BSA), the target proteins were probed with the corresponding primary antibodies overnight at 4 $^{\circ}$ C: tyrosine hydroxylase (TH), phospho-nuclear factor κ B (p-NF- κ Bp65 (Ser536)), nuclear factor κ B (NF- κ Bp65), DJ-1, Bcl-2 associated x protein (Bax), cleaved caspase-3, phosphoinositide 3-kinase (PI3K p110 α), phospho-protein kinase B (p-AKT (Ser473)), total protein kinase B (AKT), phospho-glycogen synthase kinase-3 β (p-GSK-3 β (Ser9)), total glycogen synthase kinase-3 β (GSK-3 β) (Cell Signaling Technology, USA). β -Actin was used as the loading control for the whole tissue lysate, whereas lamin B served as the loading control for the nuclear fraction lysate (Cell Signaling Technology, USA). Membranes were incubated with the appropriate horseradish peroxidase (HRP)-labeled secondary antibody, and the target proteins were visualized using Biorad ECL solution (Biorad, CA, USA). ImageJ software (Bethesda, MD, USA) was used for band quantification.

Histopathologic and Immunohistochemical Examinations. Formalin-fixed brain sections were trimmed and processed for paraffin embedding by dehydration in serial dilutions of ethanol, clearing in xylene, infiltration, and embedding into Paraplast tissue embedding media. 4 μ m thick sagittal brain sections were cut by a rotatory microtome for the demonstration of the striatal region. Sections were then stained with hematoxylin and eosin (H&E) for general morphological examination by the light microscope as described.⁵⁸ For the demonstration of intact and damaged neurons in the striatum, tissue sections were stained with toluidine blue (Nissl stain), then six randomly selected nonoverlapping fields per tissue section were evaluated for quantification of intact neurons in the striatum.

The striatal expression of TH and NF- κ Bp65 was assessed by the immunohistochemical staining of paraffin-embedded brain sections as reported.⁵⁹ Briefly, the deparaffinized tissue sections were pretreated with 0.03% trypsin at 37 $^{\circ}$ C for 1 h for antigen retrieval, followed by 0.3% H₂O₂ for 20 min to quench endogenous peroxidase activity. Subsequently, the tissue sections were blocked with 5% BSA for 30 min and then incubated overnight at 4 $^{\circ}$ C with a rabbit monoclonal anti-TH antibody (EP1532Y; catalog number ab137869, Abcam, MA, USA) or a rabbit polyclonal anti-NF- κ B p65 antibody (catalog number RB-1638-P0, Thermo Fisher Scientific, CA, USA), diluted 1:100 followed by washing with PBS. The sections were then incubated with HRP-conjugated secondary antibody (EnVision kit, Dako, Copenhagen, Denmark) for 20 min. After another washing, the immune reaction was detected by incubation with 3,3'-diaminobenzidine chromogen (Dako, Copenhagen, Denmark) for 15 min. After a final wash with PBS, the slides were counterstained with hematoxylin, dehydrated, and cleared in xylene for light microscopic examination. The percentage of the diaminobenzidine-immunopositive area to the total area of the microscopic field was computed for six randomly selected nonoverlapping fields per tissue section. All microscopic examinations and image analyses were performed using Leica Application module for histological analysis attached to a full HD

microscopic imaging system (Leica Microsystems GmbH, Wetzlar, Germany).

Statistical Analysis. Data were tested for normality by the Shapiro–Wilk normality test. Parametric data are expressed as the mean \pm standard error of the mean (SEM), and statistical comparisons among the means were performed by one-way analysis of variance (ANOVA), followed by Tukey's post hoc multiple comparisons test. The rearing frequency and the number of line crossings are represented as median (with interquartile range) and were statistically analyzed using Kruskal–Wallis nonparametric test, followed by Dunn's multiple comparisons test. All the statistical analyses were conducted using GraphPad Prism software, version 7.04 (San Diego, CA, USA). Variations between groups were regarded as statistically significant at $P < 0.05$.

AUTHOR INFORMATION

Corresponding Author

Nancy N. Shahin – Department of Biochemistry, Faculty of Pharmacy, Cairo University, Cairo 11562, Egypt;
orcid.org/0000-0002-9746-5335; Phone: +2
01228778550; Email: nancy.shahin@pharma.cu.edu.eg;
Fax: +2 0226190375

Authors

Hany H. Arab – Department of Pharmacology and Toxicology, College of Pharmacy, Taif University, Taif 21944, Saudi Arabia; Department of Biochemistry, Faculty of Pharmacy, Cairo University, Cairo 11562, Egypt
Marwa M. Safar – Department of Pharmacology and Toxicology, Faculty of Pharmacy, Cairo University, Cairo 11562, Egypt; Department of Pharmacology and Biochemistry, Faculty of Pharmacy, The British University in Egypt, Cairo 11837, Egypt

Complete contact information is available at:

<https://pubs.acs.org/10.1021/acschemneuro.0c00722>

Author Contributions

H.H.A. did the conceptualization. H.H.A, M.M.S., and N.N.S. did the methodology, investigation, formal analysis, and writing (original draft preparation). H.H.A. did the writing-reviewing and editing.

Notes

The authors declare no competing financial interest.

ACKNOWLEDGMENTS

The present study was sponsored by Taif University Researchers Supporting Project Number TURSP-2020/29, Taif University, Taif, Saudi Arabia (to H.H.A.). The authors acknowledge the efforts of Dr. M. Abdelrazik (Cairo University, Egypt) for his valuable assistance in histopathology and immunohistochemistry.

ABBREVIATIONS

AKT, protein kinase B; Bax, Bcl-2 associated x protein; DA, dopamine; DPG, dapagliflozin; GDNF, glial cell line-derived neurotrophic factor; GSK-3 β , glycogen synthase kinase-3 β ; HO-1, heme oxygenase-1; LB, Lewy bodies; NF- κ B, nuclear factor κ B; Nrf2, nuclear factor erythroid 2-related factor-2; PD, Parkinson's disease; PI3K, phosphoinositide 3-kinase; ROS, reactive oxygen species; SGLT2, sodium-glucose co-transporter 2; TH, tyrosine hydroxylase; TNF- α , tumor necrosis factor- α

REFERENCES

- (1) Sanders, L. H., and Greenamyre, J. T. (2013) Oxidative damage to macromolecules in human Parkinson disease and the rotenone model. *Free Radical Biol. Med.* 62, 111–120.
- (2) Schneider, S. A., and Obeso, J. A. (2014) Clinical and pathological features of Parkinson's disease. In *Behavioral Neurobiology of Huntington's Disease and Parkinson's Disease*, pp 205–220, Springer, Berlin.
- (3) Golpich, M., Amini, E., Hemmati, F., Ibrahim, N. M., Rahmani, B., Mohamed, Z., Raymond, A. A., Dargahi, L., Ghasemi, R., and Ahmadiani, A. (2015) Glycogen synthase kinase-3 beta (GSK-3 β) signaling: implications for Parkinson's disease. *Pharmacol. Res.* 97, 16–26.
- (4) Yan, M. H., Wang, X., and Zhu, X. (2013) Mitochondrial defects and oxidative stress in Alzheimer disease and Parkinson disease. *Free Radical Biol. Med.* 62, 90–101.
- (5) Goes, A. T., Jesse, C. R., Antunes, M. S., Ladd, F. V. L., Ladd, A. A. L., Luchese, C., Paroul, N., and Boeira, S. P. (2018) Protective role of chrysin on 6-hydroxydopamine-induced neurodegeneration a mouse model of Parkinson's disease: Involvement of neuroinflammation and neurotrophins. *Chem.-Biol. Interact.* 279, 111–120.
- (6) Malagelada, C., Jin, Z. H., and Greene, L. A. (2008) RTP801 is induced in Parkinson's disease and mediates neuron death by inhibiting Akt phosphorylation/activation. *J. Neurosci.* 28, 14363–14371.
- (7) Xie, C.-l., Lin, J.-Y., Wang, M.-H., Zhang, Y., Zhang, S.-f., Wang, X.-J., and Liu, Z.-G. (2016) Inhibition of Glycogen Synthase Kinase-3 β (GSK-3 β) as potent therapeutic strategy to ameliorates L-dopa-induced dyskinesia in 6-OHDA parkinsonian rats. *Sci. Rep.* 6, 23527.
- (8) Lin, L. F., Doherty, D. H., Lile, J. D., Bektesh, S., and Collins, F. (1993) GDNF: a glial cell line-derived neurotrophic factor for midbrain dopaminergic neurons. *Science* 260, 1130–1132.
- (9) Sherer, T. B., Betarbet, R., Stout, A. K., Lund, S., Baptista, M., Panov, A. V., Cookson, M. R., and Greenamyre, J. T. (2002) An in vitro model of Parkinson's disease: linking mitochondrial impairment to altered α -synuclein metabolism and oxidative damage. *J. Neurosci.* 22, 7006–7015.
- (10) Scholl-Bürgi, S., Santer, R., and Ehrlich, J. H. (2004) Long-term outcome of renal glucosuria type 0: the original patient and his natural history. *Nephrol., Dial., Transplant.* 19, 2394–2396.
- (11) Andrianesis, V., Glykofridi, S., and Doupis, J. (2016) The renal effects of SGLT2 inhibitors and a mini-review of the literature. *Ther. Adv. Endocrinol. Metab.* 7, 212–228.
- (12) Lin, B., Koibuchi, N., Hasegawa, Y., Sueta, D., Toyama, K., Uekawa, K., Ma, M., Nakagawa, T., Kusaka, H., and Kim-Mitsuyama, S. (2014) Glycemic control with empagliflozin, a novel selective SGLT2 inhibitor, ameliorates cardiovascular injury and cognitive dysfunction in obese and type 2 diabetic mice. *Cardiovasc. Diabetol.* 13, 148.
- (13) Naznin, F., Sakoda, H., Okada, T., Tsubouchi, H., Waise, T. Z., Arakawa, K., and Nakazato, M. (2017) Canagliflozin, a sodium glucose cotransporter 2 inhibitor, attenuates obesity-induced inflammation in the nodose ganglion, hypothalamus, and skeletal muscle of mice. *Eur. J. Pharmacol.* 794, 37–44.
- (14) Jabbour, S., and Goldstein, B. (2008) Sodium glucose cotransporter 2 inhibitors: blocking renal tubular reabsorption of glucose to improve glycaemic control in patients with diabetes. *Int. J. Clin Pract* 62, 1279–1284.
- (15) Lee, T.-M., Chang, N.-C., and Lin, S.-Z. (2017) Dapagliflozin, a selective SGLT2 Inhibitor, attenuated cardiac fibrosis by regulating the macrophage polarization via STAT3 signaling in infarcted rat hearts. *Free Radical Biol. Med.* 104, 298–310.
- (16) Sa-Nguanmoo, P., Tanajak, P., Kerdphoo, S., Jaiwongkam, T., Pratchayasakul, W., Chattipakorn, N., and Chattipakorn, S. C. (2017) SGLT2-inhibitor and DPP-4 inhibitor improve brain function via attenuating mitochondrial dysfunction, insulin resistance, inflammation, and apoptosis in HFD-induced obese rats. *Toxicol. Appl. Pharmacol.* 333, 43–50.
- (17) Erdogan, M. A., Yusuf, D., Christy, J., Solmaz, V., Erdogan, A., Taskiran, E., and Erbas, O. (2018) Highly selective SGLT2 inhibitor dapagliflozin reduces seizure activity in pentylenetetrazol-induced murine model of epilepsy. *BMC Neurol.* 18, 81.
- (18) El-Sahar, A. E., Rastanawi, A. A., El-Yamany, M. F., and Saad, M. A. (2020) Dapagliflozin improves behavioral dysfunction of Huntington's disease in rats via inhibiting apoptosis-related glycolysis. *Life Sci.* 257, 118076.
- (19) Millar, P., Pathak, N., Parthasarathy, V., Bjourson, A. J., O'Kane, M., Pathak, V., Moffett, R. C., Flatt, P. R., and Gault, V. A. (2017) Metabolic and neuroprotective effects of dapagliflozin and liraglutide in diabetic mice. *J. Endocrinol.* 234, 255–267.
- (20) Wicinski, M., Wodkiewicz, E., Gorski, K., Walczak, M., and Malinowski, B. (2020) Perspective of SGLT2 inhibition in treatment of conditions connected to neuronal loss: Focus on Alzheimer's Disease and ischemia-related brain injury. *Pharmaceuticals* 13, 379.
- (21) Gray, M. T., and Woulfe, J. M. (2015) Striatal blood-brain barrier permeability in Parkinson's disease. *J. Cereb. Blood Flow Metab.* 35, 747–750.
- (22) Shimizu, F., and Kanda, T. (2013) Disruption of the blood-brain barrier in inflammatory neurological diseases. *Brain Nerve* 65, 165–176.
- (23) Anandhan, A., Lei, S., Levytskyy, R., Pappa, A., Panayiotidis, M. I., Cerny, R. L., Khalimonchuk, O., Powers, R., and Franco, R. (2017) Glucose metabolism and AMPK signaling regulate dopaminergic cell death induced by gene (α -synuclein)-environment (paraquat) interactions. *Mol. Neurobiol.* 54, 3825–3842.
- (24) Han, S., Hagan, D. L., Taylor, J. R., Xin, L., Meng, W., Biller, S. A., Wetterau, J. R., Washburn, W. N., and Whaley, J. M. (2008) Dapagliflozin, a selective SGLT2 inhibitor, improves glucose homeostasis in normal and diabetic rats. *Diabetes* 57, 1723–1729.
- (25) Pang, M., Ma, L., Gong, R., Tolbert, E., Mao, H., Ponnusamy, M., Chin, Y. E., Yan, H., Dworkin, L. D., and Zhuang, S. (2010) A novel STAT3 inhibitor, S3I-201, attenuates renal interstitial fibroblast activation and interstitial fibrosis in obstructive nephropathy. *Kidney Int.* 78, 257–268.
- (26) Nassar, N. N., Al-Shorbagy, M. Y., Arab, H. H., and Abdallah, D. M. (2015) Saxagliptin: a novel antiparkinsonian approach. *Neuropharmacology* 89, 308–317.
- (27) Moreira, S., Fonseca, I., Nunes, M. J., Rosa, A., Lemos, L., Rodrigues, E., Carvalho, A. N., Outeiro, T. F., Rodrigues, C. M. P., Gama, M. J., and Castro-Caldas, M. (2017) Nrf2 activation by tauroursodeoxycholic acid in experimental models of Parkinson's disease. *Exp. Neurol.* 295, 77–87.
- (28) Inden, M., Kitamura, Y., Takeuchi, H., Yanagida, T., Takata, K., Kobayashi, Y., Taniguchi, T., Yoshimoto, K., Kaneko, M., Okuma, Y., Taira, T., Ariga, H., and Shimohama, S. (2007) Neurodegeneration of mouse nigrostriatal dopaminergic system induced by repeated oral administration of rotenone is prevented by 4-phenylbutyrate, a chemical chaperone. *J. Neurochem.* 101, 1491–1504.
- (29) Michel, H. E., Tadros, M. G., Esmat, A., Khalifa, A. E., and Abdel-Tawab, A. M. (2017) Tetramethylpyrazine ameliorates rotenone-induced Parkinson's disease in rats: involvement of its anti-inflammatory and anti-apoptotic actions. *Mol. Neurobiol.* 54, 4866–4878.
- (30) Cui, Q., Li, X., and Zhu, H. (2016) Curcumin ameliorates dopaminergic neuronal oxidative damage via activation of the Akt/Nrf2 pathway. *Mol. Med. Rep.* 13, 1381–1388.
- (31) Zhang, X.-L., Yuan, Y.-H., Shao, Q.-H., Wang, Z.-Z., Zhu, C.-G., Shi, J.-G., Ma, K.-L., Yan, X., and Chen, N.-H. (2017) DJ-1 regulating PI3K-Nrf2 signaling plays a significant role in bibenzyl compound 20C-mediated neuroprotection against rotenone-induced oxidative insult. *Toxicol. Lett.* 271, 74–83.
- (32) Anusha, C., Sumathi, T., and Joseph, L. D. (2017) Protective role of apigenin on rotenone induced rat model of Parkinson's disease: Suppression of neuroinflammation and oxidative stress mediated apoptosis. *Chem.-Biol. Interact.* 269, 67–79.
- (33) Han, B., Li, S., Lv, Y., Yang, D., Li, J., Yang, Q., Wu, P., Lv, Z., and Zhang, Z. (2019) Dietary melatonin attenuates chromium-

induced lung injury via activating the Sirt1/Pgc-1 α /Nrf2 pathway. *Food Funct.* 10, 5555–5565.

(34) Surh, Y.-J., and Na, H.-K. (2008) NF- κ B and Nrf2 as prime molecular targets for chemoprevention and cytoprotection with anti-inflammatory and antioxidant phytochemicals. *Genes Nutr.* 2, 313–317.

(35) Salazar, M., Rojo, A. I., Velasco, D., de Sagarra, R. M., and Cuadrado, A. (2006) Glycogen synthase kinase-3 β inhibits the xenobiotic and antioxidant cell response by direct phosphorylation and nuclear exclusion of the transcription factor Nrf2. *J. Biol. Chem.* 281, 14841–14851.

(36) Arab, H. H., Saad, M. A., El-Sahar, A. E., and Al-Shorbagy, M. Y. (2020) Mechanistic perspective of morin protection against ketoprofen-induced gastric mucosal injury: Targeting HMGB1/RAGE/NF- κ B, DJ-1/Nrf2/HO-1 and PI3K/mTOR pathways. *Arch. Biochem. Biophys.* 693, 108552.

(37) Joshi, N., and Singh, S. (2018) Updates on immunity and inflammation in Parkinson disease pathology. *J. Neurosci. Res.* 96, 379–390.

(38) Darabi, S., Noori-Zadeh, A., Abbaszadeh, H. A., Rajaei, F., and Bakhtiyari, S. (2019) Trehalose neuroprotective effects on the substantia nigra dopaminergic cells by activating autophagy and non-canonical Nrf2 pathways. *Iran. J. Pharm. Res.* 18, 1419–1428.

(39) Giordano, S., Darley-Usmar, V., and Zhang, J. (2014) Autophagy as an essential cellular antioxidant pathway in neurodegenerative disease. *Redox Biol.* 2, 82–90.

(40) Liu, J., Liu, W., Lu, Y., Tian, H., Duan, C., Lu, L., Gao, G., Wu, X., Wang, X., and Yang, H. (2018) Piperlongumine restores the balance of autophagy and apoptosis by increasing BCL2 phosphorylation in rotenone-induced Parkinson disease models. *Autophagy* 14, 845–861.

(41) Hattingen, E., Magerkurth, J., Pilatus, U., Mozer, A., Seifried, C., Steinmetz, H., Zanella, F., and Hilker, R. (2009) Phosphorus and proton magnetic resonance spectroscopy demonstrates mitochondrial dysfunction in early and advanced Parkinson's disease. *Brain* 132, 3285–3297.

(42) Hartmann, A., Hunot, S., Michel, P. P., Muriel, M.-P., Vyas, S., Faucheux, B. A., Mouatt-Prigent, A., Turmel, H., Srinivasan, A., Ruberg, M., Evan, G. I., Agid, Y., and Hirsch, E. C. (2000) Caspase-3: a vulnerability factor and final effector in apoptotic death of dopaminergic neurons in Parkinson's disease. *Proc. Natl. Acad. Sci. U. S. A.* 97, 2875–2880.

(43) Yue, P., Gao, L., Wang, X., Ding, X., and Teng, J. (2017) Intranasal administration of GDNF protects against neural apoptosis in a rat model of Parkinson's disease through PI3K/Akt/GSK3 β pathway. *Neurochem. Res.* 42, 1366–1374.

(44) Duka, T., Duka, V., Joyce, J. N., and Sidhu, A. (2009) α -Synuclein contributes to GSK-3 β -catalyzed Tau phosphorylation in Parkinson's disease models. *FASEB J.* 23, 2820–2830.

(45) King, T. D., Clodfelder-Miller, B., Barksdale, K. A., and Bijur, G. N. (2008) Unregulated mitochondrial GSK3 β activity results in NADH: Ubiquinone oxidoreductase deficiency. *Neurotoxic. Res.* 14, 367–382.

(46) Cen, X., Nitta, A., Ohya, S., Zhao, Y., Ozawa, N., Mouri, A., Ibi, D., Wang, L., Suzuki, M., and Saito, K. (2006) An analog of a dipeptide-like structure of FK506 increases glial cell line-derived neurotrophic factor expression through cAMP response element-binding protein activated by heat shock protein 90/Akt signaling pathway. *J. Neurosci.* 26, 3335–3344.

(47) Beurel, E. (2011) Regulation by glycogen synthase kinase-3 of inflammation and T cells in CNS diseases. *Front. Mol. Neurosci.* 4, 18.

(48) Yang, L., Guo, C., Zhu, J., Feng, Y., Chen, W., Feng, Z., Wang, D., Sun, S., Lin, W., and Wang, Y. (2017) Increased levels of pro-inflammatory and anti-inflammatory cellular responses in Parkinson's disease patients: Search for a disease indicator. *Med. Sci. Monit.* 23, 2972–2978.

(49) Morales-García, J. A., Susín, C., Alonso-Gil, S., Pérez, D. I., Palomo, V., Pérez, C., Conde, S., Santos, A., Gil, C., Martínez, A., and Pérez-Castillo, A. (2013) Glycogen synthase kinase-3 inhibitors as

potent therapeutic agents for the treatment of Parkinson disease. *ACS Chem. Neurosci.* 4, 350–360.

(50) Hedya, S. A., Safar, M. M., and Bahgat, A. K. (2018) Cilostazol mediated Nurr1 and autophagy enhancement: neuroprotective activity in rat rotenone PD model. *Mol. Neurobiol.* 55, 7579–7587.

(51) Freireich, E. J., Gehan, E., Rall, D., Schmidt, L., and Skipper, H. (1966) Quantitative comparison of toxicity of anticancer agents in mouse, rat, hamster, dog, monkey, and man. *Cancer Chemother Rep* 50, 219–244.

(52) Abdelsalam, R. M., and Safar, M. M. (2015) Neuroprotective effects of vildagliptin in rat rotenone Parkinson's disease model: role of RAGE-NF κ B and Nrf2-antioxidant signaling pathways. *J. Neurochem.* 133, 700–707.

(53) De Miranda, B. R., Fazzari, M., Rocha, E. M., Castro, S., and Greenamyre, J. T. (2019) Sex differences in rotenone sensitivity reflect the male-to-female ratio in human Parkinson's Disease incidence. *Toxicol. Sci.* 170, 133–143.

(54) Walsh, R. N., and Cummins, R. A. (1976) The open-field test: a critical review. *Psychol. Bull.* 83, 482–504.

(55) Jones, B., and Roberts, D. (1968) The quantitative measurement of motor inco-ordination in naive mice using an accelerating rotarod. *J. Pharm. Pharmacol.* 20, 302–304.

(56) Arab, H. H., Gad, A. M., Fikry, E. M., and Eid, A. H. (2019) Ellagic acid attenuates testicular disruption in rheumatoid arthritis via targeting inflammatory signals, oxidative perturbations and apoptosis. *Life Sci.* 239, 117012.

(57) Eid, A. H., Gad, A. M., Fikry, E. M., and Arab, H. H. (2019) Venlafaxine and carvedilol ameliorate testicular impairment and disrupted spermatogenesis in rheumatoid arthritis by targeting AMPK/ERK and PI3K/AKT/mTOR pathways. *Toxicol. Appl. Pharmacol.* 364, 83–96.

(58) Salama, S. A., Arab, H. H., and Maghrabi, I. A. (2018) Troxerutin down-regulates KIM-1, modulates p38 MAPK signaling, and enhances renal regenerative capacity in a rat model of gentamycin-induced acute kidney injury. *Food Funct.* 9, 6632–6642.

(59) Arab, H. H., Salama, S. A., and Maghrabi, I. A. (2018) Camel milk ameliorates 5-fluorouracil-induced renal injury in rats: Targeting MAPKs, NF- κ B and PI3K/Akt/eNOS pathways. *Cell. Physiol. Biochem.* 46, 1628–1642.